68th International Astronautical Congress (IAC), Adelaide, Australia, 25-29 September 2017.


IAC-17- D2.4.3

# Evaluation of Future Ariane Reusable VTOL Booster stages

**Etienne Dumont[a]*, Sven Stappert[a], Tobias Ecker[b], Jascha Wilken[a], Sebastian Karl[b], Sven Krummen[a], Martin Sippel[a]**

[a] *Department of Space Launcher Systems Analysis (SART), Institute of Space Systems, German Aerospace Center (DLR), Robert Hooke Straße 7, 28359 Bremen, Germany*
[b] *Department of Spacecraft, Institute of Aerodynamics and Flow Technology, German Aerospace Center (DLR), Bunsenstraße 10, 37073 Gottingen, Germany*
*etienne.dumont@dlr.de

## Abstract

Reusability is anticipated to strongly impact the launch service market if sufficient reliability and low refurbishment costs can be achieved. DLR is performing an extensive study on return methods for a reusable booster stage for a future launch vehicle. The present study focuses on the vertical take-off and vertical landing (VTOL) method. First, a restitution of a flight of Falcon 9 is presented in order to assess the accuracy of the tools used. Then, the preliminary designs of different variants of a future Ariane launch vehicle with a reusable VTOL booster stage are described. The proposed launch vehicle is capable of launching a seven ton satellite into a geostationary transfer orbit (GTO) from the European spaceport in Kourou. Different stagings and propellants (LOx/LH2, LOx/LCH4, LOx/LC3H8, subcooled LOx/LCH4) are considered, evaluated and compared. First sizing of a broad range of launcher versions are based on structural index derived from existing stages. Ascent and descent trajectories of the first stage are optimized together in order to reach the highest payload while keeping mechanical loads at reasonable levels. Another important aspect is the aerothermal environment stressing the structure. During the re-entry boost, the first stage is immersed in the engine exhaust plume. Steady state computational fluid dynamics calculations are performed along the re-entry trajectory to characterise the flow field during retro-propulsion around the first stage. The resulting aerothermal database is coupled with a simple structural model to study the time dependent heating of the hull structure. Based on these first iteration results more detailed preliminary designs are performed in a second iteration for selected configurations: a LOx/LH2 launcher and a LOx/LCH4 launcher both equipped with gas generator engines.

**Keywords:** Ariane, reusability, toss-back, vertical landing, VTOL, VTVL, liquid hydrogen, liquid oxygen, liquid methane, liquid propane, subcooled methane, gas generator, staged combustion, RTLS, DRL

## Nomenclature

| | | |
|---|---|---|
| $C_D$ | Drag coefficient | - |
| $C_p$ | Heat capacity | J/kgK |
| Isp | Vacuum specific impulse | s |
| F_vac | Engine vacuum thrust | kN |
| MR | Engine mixture ratio | - |
| M_sep | Separation Mach number | - |
| Pcc | Combustion chamber pressure | bar |
| Re | Reynolds number | - |
| ΔV | Velocity increment | km/s |
| ε | Expansion ratio | - |

## Acronyms/Abbreviations

| | |
|---|---|
| 3-STO | Three Stages to Orbit |
| ASDS | Autonomous Spaceport Droneship |
| DRL | Down-Range Landing |
| ELV | Expendable Launch Vehicle |
| GG | Gas Generator cycle engine |
| GTO | Geostationary Transfer Orbit |
| LCH4 | Liquid Methane |
| LC3H8 | Liquid Propane |
| LH2 | Liquid Hydrogen |
| LOx | Liquid Oxygen |
| MECO | Main Engine Cut-Off |
| MR | Mixture Ratio |
| Mg | Mega gram or metric ton |
| NBP | Normal Boiling Point |
| NTP | Near Triple Point |
| Prop. | Propellant |
| RLV | Reusable Launch Vehicle |
| RTLS | Return To Launch Site |
| SC | Staged Combustion cycle engine |
| TP | Triple Point |
| TSTO | Two Stages To Orbit |
| VTOL | Vertical Take-Off and Landing |
| VTL | Vertical Take-Off and Landing = VTOL |

## 1. Introduction

With the success of Blue Origin (New Shepard) and SpaceX (Falcon 9) in recovering and reusing a stage by

retro-propulsion, the need to develop a partly reusable launch vehicle in Europe is increasing. It might be a key element to keep a leading position in the commercial launch service market in the future.

Numerous studies of reusable or partly reusable launch systems have been performed in the past at DLR. Several of them considered winged first stages or boosters equipped with air-breathing engines, such as the ASTRA Liquid Fly Back Booster concept [1]. The goal was the replacement of the solid rocket motors of the Ariane 5 with newly developed cryogenic reusable boosters, in order to increase performance and reduce launch service costs. At MECO these boosters should first perform an atmospheric re-entry followed by an aerodynamically controlled turn to return towards the launch site. After the turn the air-breathing engines are switched-on and a flight back to the launch site is performed with optimal fuel consumption. The landing is then performed horizontally on a runway. This method has the drawback that all systems and propellant required for the return have to be carried from lift-off. This adds mass and complexity to the system compared to a classic ELV first stage. To partially solve this problem an innovative solution has been proposed and patented: the so called In-Air Capturing method [2] and [3]. The stage is equipped as in the case of the fly-back with a wing, but neither engines, nor propellants for the fly-back are needed. This has a strong positive impact on the vehicle mass at separation. After the atmospheric re-entry, the returning stage is captured in flight by an unmanned plane. It is then towed back close to the launch site, where it lands as a glider. This concept has the big advantage of reduced mass at stage separation and also allows the decoupling of the optimisation of the ascent from the optimization of the return flight. Contrary to this approach, for the fly-back method, the optimisation of the ascent cannot be performed completely independently of the return flight. Indeed for a better payload performance, if the descent is not considered, it is advantageous not to fly too steep, i.e. to reduce the flight path angle as early as possible. This leads to a comparatively large down-range and horizontal velocity at stage separation and therefore increases the propellant required for the return flight. While LFBB requires only a runway, in-air capturing requires in addition a plane to tow the booster stage.

The retro-propulsion method is very different from the aforementioned methods, as propulsion is the main element to control the descent. After the stage separation, several engine boosts allow the stage to target a predefined landing area, reduce the re-entry velocity to limit thermal and structural loads and finally perform a soft vertical landing. This method is not new, as it was already tested under the Delta Clipper program [4]. But its use on an operational launcher could have a significant impact on the launcher market. DLR has been monitoring and analysing the technological advances made by SpaceX ([5], [6], [7], [8] and [9]) with regards to this return method.

The retro-propulsion method has been demonstrated and seems particularly well adapted to the market Space X is targeting. However the European situation with a smaller institutional market and mainly GTO satellites to be launched does not necessarily require a launch vehicle based on the same return method. In order to assess which method would be the most suitable for a future partly reusable European launch vehicle, a system study has been initiated to compare the fly-back method, the in-air capturing method, the retro-propulsion with return to launch site (RTLS) and the retro-propulsion with down–range landing (DRL). While these return methods have been already studied independently, the present system study is based on completely new sizing using the same starting assumptions. The following preliminary requirements and assumptions are considered:

- Design mission: launch 7000 kg to GTO
- GTO: 250 km x 35786 km, 6°
- Launch site: Europe's Spaceport, Kourou
- Project margin 500 kg
- TSTO: Two-Stage to Orbit
- Same propellant combination in both stages
- Same engines in both stages with exception of the nozzle extension

Note that the combination of a TSTO with a GTO reference mission is sub-optimal if the goal is to keep the size of the vehicle limited. TSTO launch vehicles are much better suited for LEO missions. A 3-STO could in most cases be built smaller for a GTO reference mission. However, it would be more difficult to use the same motor for each stage. In this study, the goal is not to present an optimized GTO launcher, but to compare reusability methods and the influence of the propellant combination for generic launchers performing a GTO reference mission. Selecting a TSTO concept limits the influence of external parameters (i.e. not related to the reusability method) such as the staging or thrust level of the second and a potential third stage.

Some preliminary results for the fly-back and the in-air capturing methods with similar requirements and assumptions have been presented by Bussler et al. in [10]. The present paper focuses on the retro-propulsion method and thus on vertical take-off and landing. Both the RTLS (three boosts) and down-range landing (DRL) (i.e. barge landing with two boosts) have been the object of preliminary analyses. Several propellant combinations have been considered in order to verify their impacts at system level. Liquid oxygen has been considered in combination with liquid hydrogen as well as with liquid methane and liquid propane which are expected to have some operational advantages and a

greater density. Near triple point LOx/LCH4 is also considered. For each propellant combination gas generator cycle engines have been evaluated. The staged combustion cycle has been considered only for the LOx/LH2 at this stage of the study.

## 2. Method and validation

### *2.1 Trajectory optimisation method*

The 3DOF (degree of freedom) trajectory simulation and optimisation has been performed with the help of the DLR in house program *tosca* [11]. It is able to optimise ascent trajectory and powered descent trajectories separately. *Tosca* is based on an SLSQP (Sequential Least Squares Programming) optimizer and an 8th-order Runge-Kutta method solver.

The combined optimisation of the ascent and the descent is performed with the help of DLR's *rts* software [11], which links the ascent with the descent trajectory optimisation. The optimal combination of ascent and descent is indeed not necessarily obtained for the optimal ascent trajectory. Indeed parameters such as the altitude, position, velocity and flight path angle of the first stage at first MECO have a strong influence on the amount of propellant required for the descent/return. In particular, a flatter ascent trajectory leads to a higher horizontal velocity at MECO. Usually flat trajectories allow reducing the gravity losses and therefore have higher performances than steeper ascents. But in the case of the RTLS, for instance, the horizontal velocity has to be eliminated before the stage can start flying back towards the launch site. In this case, a too flat ascent leads to higher propellant requirement for the descent and consequently lower performances.

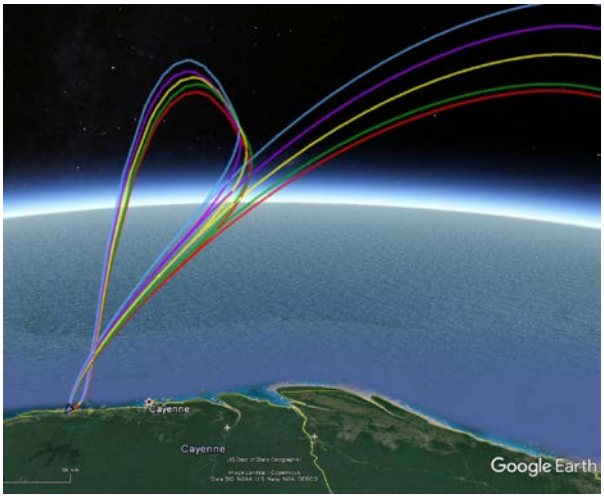


Fig. 1. Example of combined ascent and RTLS trajectory computed with tosca and rts. (image generated with Google Earth, image data: US Dept of State Geographer, Landsat/Copernicus, Data SIO, NOAA, US Navy, NGA GEBCO)

Since the pitching rate is the parameter that influences the ascent trajectory the most it is varied parametrically. For each studied pitching rate a couple of optimised ascent and descent trajectories have been calculated and the performances computed. This parametric variation allows the relatively quick determining of the highest performance for a given configuration performing a RTLS or a DRL. An example of such a pitching rate variation is shown in Fig. 1.

Both RTLS and DRL are considered. In the case of RTLS, three boosts are needed. First, shortly after MECO, the first stage turns by almost 180° and engines are ignited in order to redirect the stage towards the landing site. After a ballistic phase a re-entry boost is performed to decrease the re-entry velocity and thus decrease the loads on the vehicle while arriving in the denser layer of the atmosphere. Finally shortly before reaching the ground, one or several engines are ignited to brake and control the stage until it lands smoothly on ground. In the case of the DRL, it has been considered that the landing zone, for instance, a barge is always placed in the plane of the ascent. Consequently the first boost needed for the RTLS is not needed for DRL.

### *2.2 Validation with help of Falcon 9 flights*

Prior to the analysis of the Ariane VTOL launchers, extensive studies of the SpaceX launcher: Falcon 9 and several of its actually flown missions were analysed to gain a better understanding of the impact of the non-winged VTOL method on the launcher's performance. Therefore, different mission trajectories were calculated with the DLR in-house tool *tosca* and were compared to telemetry data provided by the SpaceX launch webcasts. The Falcon 9 was modelled using DLR tools: *pmp* for the propellant system, *lsap* for the structure, *cac* for the aerodynamics and *stsm* for the mass estimation [8]. By comparing the trajectories calculated using *tosca* with the data from the launch webcasts, descent propellant masses and performance estimations can be derived. Furthermore, a simplified structural model of the Falcon Heavy was set up and trajectories and performances were calculated respectively.

Fig. 2 shows the trajectory of the first stage of the NROL-76 mission from 30th April 2017. The first stage performed a successful RTLS landing after MECO and stage separation. The second stage continued to carry a classified satellite to LEO. The webcast provided by SpaceX supplied telemetry data for the ascent and the whole descent of the first stage, thus rendering it very useful to validate the Falcon 9 model and the tossback trajectory calculation. Fig. 2 shows a great accordance of the actual trajectory (labelled as 'webcast') and the DLR calculated trajectory ('tosca'). Hence, the assumptions and the launcher model used seem to be accurate enough and the respective performances

calculated shall be quite close to the actual launcher. Furthermore, for the Ariane VTOL it means that the same method can be used to accurately assess the propellant needed for the return flight and consequently the launcher performances.

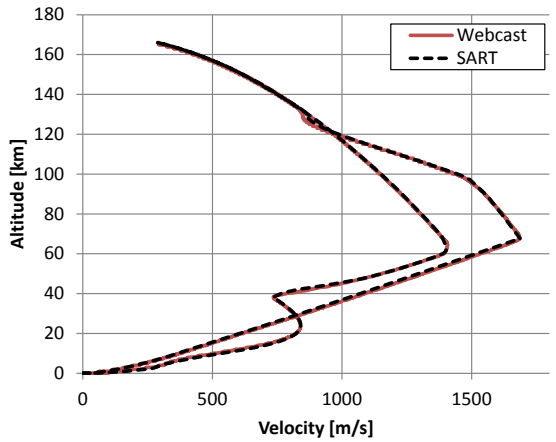


Fig. 2. Altitude over velocity of Falcon 9 1st stage during ascent and descent of the NROL-76 mission on 30th April 2017

The estimated payload performance reduction of the Falcon 9 when operated as RLV is high. For a LEO mission with barge landing (DRL) the payload performance is reduced by 30%-35% compared to a Falcon 9 used as ELV. For LEO missions with RTLS the payload performance reduction is even estimated to be between 60%-65% [8]. This can be explained by the fact that RTLS landings require more energy to revert the horizontal velocity of the first stage after MECO to set it on a trajectory back to the launch site. The required energy is delivered by the descent propellant, thus lowering the maximum possible payload performance. In addition the ascent trajectory is made steeper to reduce the horizontal velocity at MECO, this however increases the gravity losses during the ascent.

Furthermore, performance losses using barge landings for missions to GTO are around 30%-35%, similar to LEO missions with barge landing. Actually, performance losses should be higher for the GTO mission since the final orbit is more energetic. For this reason, SpaceX, uses only two burns instead of three burns (as they do for all LEO return missions) to land the first stage on a barge during GTO missions. Thus, the required descent propellant mass and performance losses can be lowered. The re-entry conditions for GTO missions are however harsher with only two boosts, as shown in Fig. 3.

In summary, performance losses are high when using the retro-propulsion VTOL method to land first stages either on land or on a barge down-range. This leads to an increase of total lift-off mass compared to ELV launchers with the same payload capacity. The Falcon Heavy is capable of delivering 24 tons to LEO when operated as RLV which is roughly comparable to the LEO payload capability of the Ariane 5 (~20 tons) The gross lift-off mass (GLOM) of the Falcon Heavy (1410 tons) is almost twice as high as the GLOM of the Ariane 5 (~780 tons). This difference cannot be explained entirely by the different propellant used. Despite this, the retro-propulsion VTOL method provides high flexibility by enabling different operation modes (RLV/ELV, DRL/RTLS) according to the required mission and payload mass. This allows SpaceX to perform a large range of missions with a unique launcher.

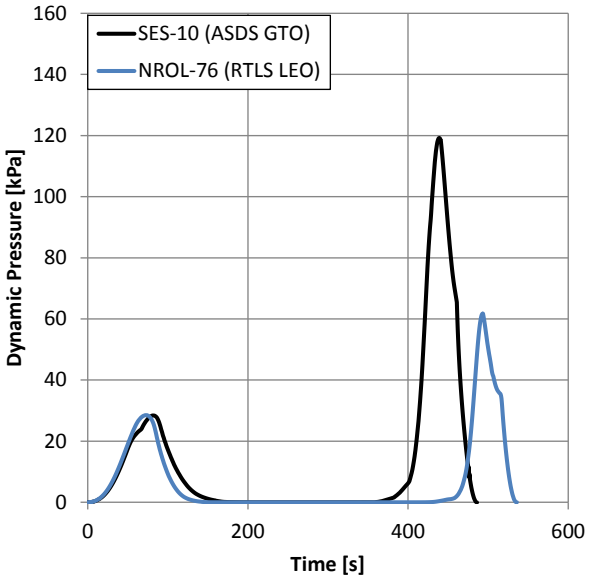


Fig. 3. Dynamic pressure over time for Falcon 9 first stage descent trajectories of SES-10 and NROL-76 mission

## 3. Vehicle design

The Ariane VTOL vehicle preliminary design has been performed iteratively. In a first iteration, a simplified model has been built. The mass of the stages has been estimated using structural index curves, derived from existing stages.

### *3.1 Propellants*

Different propellants have been considered during this study. The baseline propellant combination is LOx/LH2 which has a long heritage within the European aerospace industry. Additionally, hydrocarbon fuels are also considered. While kerosene has played a major role in the past for rocket propulsion, methane has recently been receiving a lot of attention. The advantage of the higher specific impulse of LCH4/LOx over RP1/LOx is only valid at engine level, however at system level it is counterbalanced by the higher density of RP1/LOx [12]. For reusability, LCH4/LOx is a good alternative as cocking problems in the regenerative circuit are not present [13]. Another alternative is liquid propane (LC3H8). It has the advantage of being almost

40% denser than methane, at the cost of a slightly lower specific impulse. The risk of cocking is almost inexistent as it occurs for temperatures above 730 K, which is the upper limit of the coolant-side wall temperature [13]. The main thermodynamic properties of these propellants at normal boiling point and near triple point are summarized in Table 1. Propellant sub-cooling is a possible approach to increase the storage density. The density of LOx and LH2 can be increased by 14.5% and 8.8% respectively at near triple point conditions. For methane and propane the increase in density are 8.3% and 26%, respectively.

Table 1. Properties of selected propellant [14], [15]

| Prop. name | Temp. [K] | Density [kg/m³] | NBP [K] | NTP [K] |
|---|---|---|---|---|
| LOx | 90 | 1142.1 | 90 | 54.3 |
| LCH4 | 111.6 | 422.9 | 111.6 | 90.8 |
| LC3H8 | 231.1 | 581.5 | 231.1 | 85.7 |
| LH2 | 20.3 | 70.8 | 20.3 | 14 |
| TPOx | 54.4 | 1308 | - | - |
| TPCH4 | 90.7 | 458 | - | - |
| TPC3H8 | 85.5 | 733.1 | - | - |
| TPH2 | 13.8 | 77 | - | - |

The effective bulk density for normal boiling point propellant combinations and near triple point propellant combinations are shown in Table 2 for mixture ratios determined for the gas generator engines of section 3.2. It can be observed that sub-cooling LH2/LOx and LCH4/LOx to near triple point increases the bulk density by 10% to 11%. In the case of LC3H8/LOx, the density increase can reach up to 20%. Therefore LC3H8/LOx has a large potential for densification and if densification is implemented as an evolution of an existing launch vehicle, LC3H8/LOx offers the largest potential for performance growth.

Table 2. Bulk density of propellant combinations

| Propellant combination | MR [-] | Bulk Density [kg/m³] |
|---|---|---|
| LH2 / LOx | 5.8 | 354.1 |
| LCH4 / LOx | 2.52 | 770.1 |
| LC3H8 / LOx | 2.15 | 874.5 |
| TPH2 / TPOx | 5.8 | 390.3 |
| TPCH4 / TPOx | 2.52 | 856.4 |
| TPC3H8 / TPOx | 2.15 | 1047.3 |

In order to assess the performance increase through densification, the combination of TPCH4/TPOx was investigated alongside the regular LCH4/LOx launchers. For these investigations it was assumed in the first iteration that the engine performance and size is identical to an equivalent engine using NBP-propellants. Upcoming studies will look at LOx/LC3H8 and LOx/LH2 densification.

*3.2 Engines*

A preliminary system design of the engine has been performed with the help of the DLR in-house tool lrp. The design considered the fact that the engine should be reusable through a limitation of the temperature at the inlet of the turbines. A maximum of 780 K has been set, in order to avoid too high thermal loads on the turbine blades. The mixture ratio has been chosen correspondingly.

For the gas generator cycle engines, the gas generator is burning a fuel rich mixture at a pressure of 110 bar. The main combustion chamber pressure is set at 120 bar similar to the Vulcain 2 engine, which has a demonstrated test bench life-time of over 10000 seconds during 20 cycles [16]. The staged combustion cycle engine is derived from the SpaceLiner main engine described in [17]. The combustion chamber pressure of this full flow staged combustion engine is set to the relatively low pressure of 160 bar.

The estimation of the lifetime of an engine depends on many parameters. In particular the thermal but also mechanical loads on the turbine and on the regeneratively cooled thrust chamber have a strong impact on life-time. Results presented in [18] show that gas generator cycle engines have some advantages compared to other cycles for reusability. Increasing the number of cycles before failure for a staged combustion engine to the level of a gas generator engine would be possible, at the cost of reduced performances.

In order to allow for a soft landing, the engines should be throttleable. A maximal throttling level of 30% has been allowed, 100% being the nominal thrust. The minimum throttling level has been selected based on test results obtained with the advanced porous injector (API) [19]. Coaxial injectors do not normally show an efficient behaviour at very deep throttling levels. Note that depending on the studied concepts, the engine does not necessarily need to be throttled down so far for the landing. This throttling level was considered when choosing the expansion ratio, as flow separation in the nozzle even in case of deep throttling at landing, should be avoided. During landing, an exit nozzle pressure over 0.3 bar at a thrust/stage weight ratio of 1 should guarantee the absence of flow separation. For the first stage an expansion ratio of 20 for the gas generator engines was selected. For the staged-combustion engine running on a higher main combustion chamber pressure, an expansion ratio of 23 has been selected. The upper stage engine is always identical to the first stage engine but equipped with a nozzle with an expansion ratio of 180. No optimization of the expansion ratio has been performed.

The engine mixture ratio has been optimized in order to reach the highest possible specific impulse, except in the case of LOx/LH2. Since the specific impulse in that case has a very flat optimum a

compromise has been sought in order to keep the bulk density at an acceptable value while still achieving a high Isp.

The main characteristics of these engines are summarized in Table 3.

Table 3. Engine main characteristics

| Engine designation | LH2 SC | LH2 GG | LCH4 GG | LC3H8 GG |
|---|---|---|---|---|
| Cycle | Staged Comb. | Gas generator | | |
| Propellant | LOx / LH2 | | LOx / LCH4 | LOx / LC3H8 |
| Engine MR [-] | 6.0 | 5.8 | 2.52 | 2.15 |
| Main chamber MR [-] | 6.0 | 6.86 | 3.38 | 2.95 |
| Pcc [bar] | 160 | 120 | | |
| GG/Preburner pressure [bar] | Fuel-rich: 323 Ox-rich: 319 | 110 | | |
| Isp s.l. ε=20 [s] | 394.4 (ε=23) | 366.3 | 302.5 | 298.4 |
| Isp vac. ε=20 [s] | 428.6 (ε=23) | 404.7 | 334.1 | 329.6 |
| Isp vac. ε=180 [s] | 463.9 | 445.7 | 369.2 | 364.3 |

*3.3 Preliminary design assumptions*

For the first iteration loop, the dry mass of the stages has been assessed based on structural index curves. First data from existing and past stages has been gathered. Data can be found in particular for LOx/LH2 and LOx/kerosene stages and trend lines drawn. No operational stage has been built until now for the LOx/LCH4 and LOx/LC3H8 propellant combinations. The bulk density of LOx/LCH4 and LOx/LC3H8 is however situated between the ones of LOx/LH2 and LOx/kerosene. Therefore structural index curves have been interpolated based on the bulk density of the different propellant combination. The resulting structural index curves can be seen in Fig. 4. As expected the larger the bulk density, the lower the structural index.

Engine masses have been estimated separately with the help of the lrp software. The mass of the equipment required for the descent such as the grid fins and the landing legs have been scaled from the model of the Falcon 9 launch vehicle. For the preliminary design the landing mass is taken as reference for the scaling. The mass of reserve and residual propellants have been determined based on experience.

Up to three different stagings have been considered for each propellant combination. A possible way to set the staging is to choose a Mach number for the separation of the first stage. This might be interesting in cases where the focus lies on comparing thermal protection systems. But the speed of sound depends on the altitude. Therefore for a given vehicle, the separation Mach number will vary strongly with the altitude reached. This altitude, itself can change strongly with the selected ascent trajectory. Thus this metric was not used within this study.

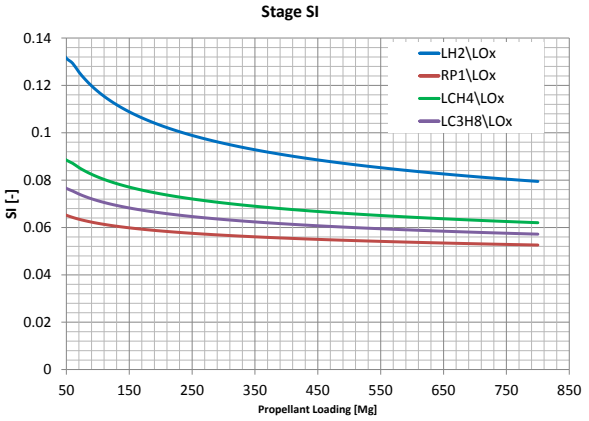


Fig. 4. Structural index curve (without engine) for different propellant combination

In this study, the ΔV provided by the upper stage has been selected as the metric for defining the staging. The objective is indeed the comparison of first stage reusability methods. For this purpose, upper stage designs independent of the reusability method are considered. The selected upper stage ΔV have been derived from preliminary designs performed for the fly-back return method and presented in [10]. They are the following:

- 6.6 km/s (corresponding to Mach 12 for fly-back)
- 7.0 km/s (corresponding to Mach 9 for fly-back)
- 7.6 km/s (corresponding to Mach 6 for fly-back)

## 4. Resulting preliminary design from first iteration

*4.1 RTLS method*

In the case of the first stage returning to the launch site and launching 7 to 7.5 tons to GTO, large stages were expected. As a comparison, Falcon 9 does not perform a RTLS for GTO missions; at best it performs a barge landing and even that only for lighter payloads.

*4.1.1 LOx/LH2 Gas generator*

In the case of LOx/LH2 with gas generator engines and an upper stage ΔV of 7.6 km/s, corresponding to the lower first stage separation velocity and therefore the smallest ΔV to return to launch site, the preliminary design converged towards a H1000H250. In other words, the first stage would have a propellant loading of 1000 tons, of which 810 tons are required for the ascent and 190 tons needed for the RTLS. This is about 30% larger than the core stage of the Energia launch vehicle, which is the largest LOx/LH2 stage built until now. The upper stage itself would carry 250 tons of LOx/LH2 or 50% more than the Ariane 5 EPC core stage. The gross

lift off mass in this case would be slightly over 1.4 Gg or twice as heavy as the Ariane 5. The economic relevance of such a large vehicle is questionable.

If the ΔV of the upper stage is reduce to 7.0 km/s, its size decreases substantially to a propellant loading of 140 tons. The first stage at separation is however faster and higher, thus a higher ΔV is required to bring back the stage to the launch site. Consequently the first stage needs to carry 1300 tons of LOx/LH2. 1020 tons are needed for the ascent and 280 tons are needed for the return to launch site. In this case the recovered first stage is larger, but the vehicle is even larger and the economic relevance of such a large vehicle does not seem to be much higher.

#### *4.1.2 LOx/LCH4 Gas generator*

The preliminary sizing of a LOx/LCH4 version with a first stage performing a RTLS has been performed for the upper stage ΔV of 7.6 km/s. Due to the lower specific impulse compared to the LOx/LH2 propellant combination the first stage propellant loading has to reach 3020 tons of which about 500 tons are needed for the RTLS. The upper stage propellant loading has been estimated to be 450 tons, or larger than the first stage of Falcon 9. Once again the relevance of a launcher with a gross lift-off mass of about 3800 tons is very questionable.

#### *4.1.3 First conclusions from preliminary sizing for the RTLS method*

No further preliminary sizing has been performed for the RTLS method. As it could be expected the launchers reach sizes that are not compatible with a competitive operation of the vehicles. As already mentioned in the introduction, the TSTO architecture is suboptimal for a GTO mission. It leads to a large upper stages which themselves require larger first stages to be accelerated. Note as well that the first iteration preliminary designs are based on pre-assumed structural index. In the range of tankage of the solutions presented, few historical data points are available. A structural sizing is therefore needed in a subsequent iteration to check the sizing.

If the propellant combinations are compared, the LOx/LH2 can be built a bit compacter than the LOx/LCH4 versions. The higher density of LOx/LCH4 combination is not able to compensate for the larger required propellant loading. Another interesting result concerns the number of engine required in the first stage. It can be lower for the LOx/LH2 version as the ratio between the launch mass and the landing mass is not as high as in the case of the LOx/LCH4 version. The LOx/LH2 version is lighter at launch and has a higher structural index. In the present design for the upper stage ΔV of 7.6 km/s the LOx/LH2 launcher requires 9 engines in the first stage whereas 18 are required for LOx/LCH4.

### *4.2 DRL method*

In the case of the barge landing, launching 7 to 7.5 tons to GTO seems feasible with a reasonably large launcher, when looking at Falcon 9 performances and considering the advantage of a launch from Kourou at only 5.14° north from the equator.

An overview of the generic launchers pre-sized with the help of the pre-assumed structural index is proposed in Table 4. The denomination of the launcher is as follows. One or two letters indicate the propellant combination H for LOx/LH2, C for LOx/LCH4, PR for LOx/LC3H8. It is followed by the stage propellant tankage in tons. H565H130 is therefore a TSTO with both stages running on LOx/LH2 and with 565 tons and 130 tons of propellant in the first stage and the second stage respectively. More details about the preliminary sizing are given in the following subsections.

Table 4. Overview of DRL launchers sized with the structural index method

| Prop. | engine type | upper stage ΔV [km/s] | | |
|---|---|---|---|---|
| | | 6.6 | 7 | 7.6 |
| LH2/LOx | GG | H585H100 | H565H130 | H645H235 |
| | SC | H425H80SC | H435H110SC | H470H185SC |
| LCH4/LOx | GG | C1198C170 | C1250C245 | C1999C672 |
| LC3H8/LOx | GG | PR1200PR160 | PR1230PR230 | PR2000PR660 |
| subcooled LCH4/LOx | GG | *not calculated* | TPC960TPC215 | *not calculated* |

#### *4.2.1 LOx/LH2 Gas generator*

TSTO launch vehicle with a first stage performing a DRL and propelled by gas generator LOx/LH2 engines can be built much smaller than for the RTLS method. The smallest launcher obtained in this case is H585H100, which upper stage provides 6.6 km/s to the payload, see Fig. 5.

For a larger upper stage ΔV of 7.0 km/s, the upper stage grows by 30% and reaches H130. However, the lower stage does not become much smaller, although it has to provide a significantly smaller ΔV. This is caused by the need to accelerate a larger upper stage. The propellant loading of the first stage decreases from 585 tons to 565 tons, about 3.5%. This phenomenon is even more marked for an upper stage ΔV of 7.6 km/s. The upper stage needs to be even larger: H235. It implies a growth of the lower stage, H645, which does provide a ΔV 1 km/s smaller than H585 but has to accelerate a much larger upper stage. The gross lift off masses for the two smallest versions is situated around 800 tons which is comparable with Ariane 5. They are relying on engines comparable to Vulcain 2. Nine engines with short nozzles are required in the first stage and one with a larger nozzle in the second stage. The

descent propellant mass is in every cases around 50 tons and proportionally higher for a higher separation velocity.

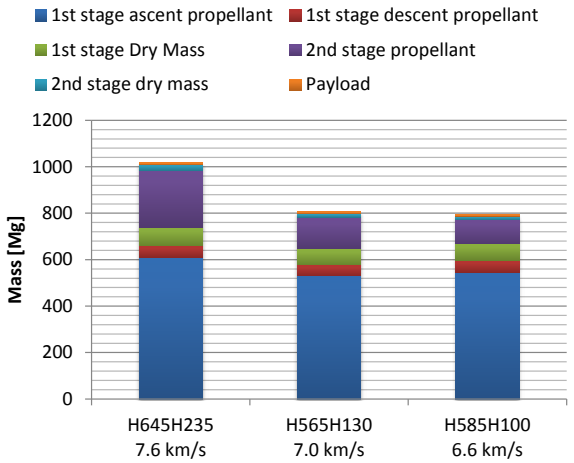


Fig. 5. Overview of the preliminary LOx/LH2 gas generator configurations

*4.2.2 LOx/LH2 Staged combustion*

As expected, if staged combustion engines are used instead of gas generator engines the size of the vehicle can be decreased further. The lightest variant is the one for which the upper stage provides the smallest ΔV: H425H80 with just over 600 tons gross lift-off mass, see Fig. 6.

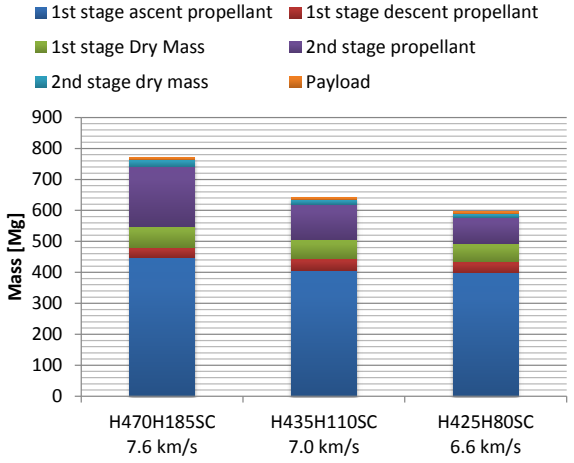


Fig. 6. Overview of the preliminary LOx/LH2 staged combustion configurations

If the ΔV provided by the upper stage increases, its size increases but as for the gas generator version the lower stage which has to provide a smaller ΔV is not getting smaller. It can even increase in size, when the upper stage becomes too large. In the case of the H470H185 it appears that reducing the number of engines to 7 in the first stage is advantageous for the upper stage as each single engine has then a higher thrust level, and the gravity losses for the upper stage decrease. For the two other preliminary designs, 9 engines with about 1 MN vacuum thrust are sufficient for the first stage. It appears from the preliminary design that the vehicles with staged combustion engines are about 25% lighter at launch than those with gas generator engines.

*4.2.3 LOx/LCH4 Gas generator*

The results of the preliminary design study for the LOx/LCH4 gas generator launchers with DRL of the first stage are shown in Fig. 7. Two of the designs corresponding to the lowest ΔV for the upper stage have a GLOM in the same order of magnitude as the Falcon Heavy, with a small advantage for the version with an upper stage ΔV of 6.6 km/s. The GLOM is then just above 1500 tons.

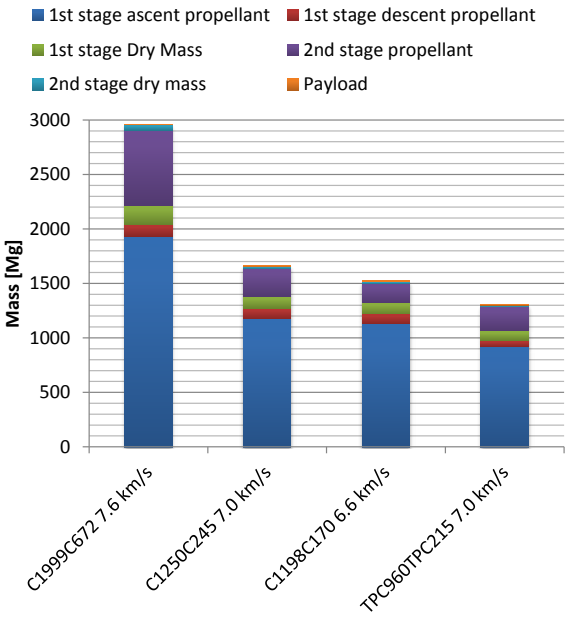


Fig. 7. Overview of the preliminary LOx/LCH4 and subcooled LOx/LCH4 gas generator configurations

Generally, the launchers with 6.6 km/s and 7.0 km/s of upper stage ΔV are about twice as heavy as the respective LOx/LH2 gas generator launchers from Fig. 5. However, the launcher with an upper stage ΔV of 7.6 km/s is almost three times heavier than the respective LOx/LH2 launcher. The GLOM of the 6.6 and 7.0 km/s version are not too far apart, while the increase in GLOM of the 7.6 km/s compared to the 7.0 km/s version is about 80%. Therefore, it appears that the descent propellant mass increases with increasing ΔV of the second stage. The descent propellant mass is mainly driven by two counteracting effects; on the one hand, a higher ΔV of the second stage leads to a lower separation velocity of the first stage. Hence, less propellant is needed to decelerate the first stage to terminal landing velocity. On the other hand, a higher ΔV of the second stage leads to heavier stages, thus increasing the amount of propellant needed to

decelerate. As for the methane launchers, the latter effect is of higher influence on the descent propellant mass required, while the hydrogen launchers show a different behaviour of almost constant descent propellant mass, regardless of ΔV of the second stage. Note that these results are highly linked to the chosen structural index curves. When the number of engines is considered, one can remark that it varies between 9 and 15. A smaller number of engines is advantageous for high upper stage ΔV. The upper stage engine then has more thrust and the gravity losses during the flight of the upper stage are lower. In the case of the lower ΔV for the upper stage, a too powerful upper stage engine penalizes the performances with its mass. On the other hand, the first stage requires a good thrust/weight ratio at launch and the possibility to almost hover at landing without throttling down too low. A larger number of engines then becomes advantageous.

*4.2.4 LOx/LC3H8 Gas generator*

The preliminary design results for the LOx/LC3H8 gas generator TSTO with the first stage performing DRL are summarized in Fig. 8.

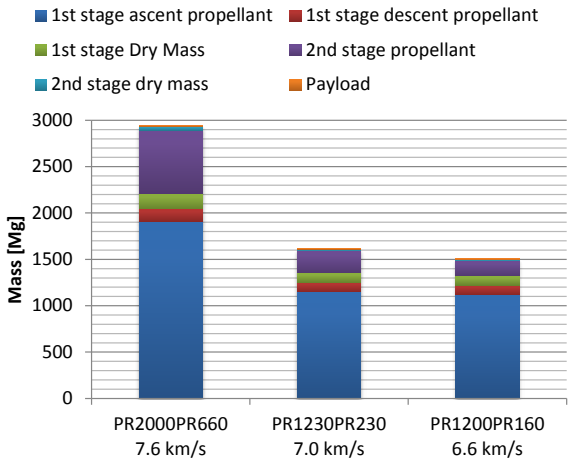


Fig. 8. Overview of the preliminary LOx/LC3H8 gas generator configurations

The lightest vehicle is the one for which the ΔV provided by the upper stage is the smallest: 6.6 km/s. This vehicle, a PR1200PR160, has a gross lift-off mass, slightly above 1500 tons, that is to say similar to the future Falcon Heavy launch vehicle of SpaceX. It is equipped with 13 engines, as is the version with an upper stage providing 7.0 km/s ΔV. As noted for the previous propellant combinations, a higher upper stage ΔV leads to larger upper and lower stages. The reason is the same for the propane launchers. The phenomenon is especially significant for an upper stage ΔV of 7.6 km/s. In this case the vehicle gets almost twice as large as for an upper stage ΔV of 6.6 km/s.

When compared to the LOx/LCH4 combination, it appears that whereas the specific impulse achievable with LOx/LC3H8 is lower, the final stage size is very close, with even a small advantage for LOx/LC3H8. This is made possible by the higher density of LC3H8 compared to LCH4, leading to a smaller structural index. The launchers are therefore at least 13.5% smaller in volume for the LOx/LC3H8 combination.

*4.2.5 TPOx/TPCH4 Gas generator*

As mentioned in section 3.1 a densified configuration was also investigated within the scope of this study. Since this was not the core of the study only a single upper stage ΔV was considered. Fig. 7 shows the results of the investigation alongside the NBP-LOx/LCH4 launchers.

The results indicate large possible reductions of the rockets size and mass when using densified propellants. The GLOM of the version with an upper stage ΔV of 7.0 km/s is about 1300 Mg. In comparison to the NBP-version the GLO mass of the NTP-version is reduced by about 21 % and the tank volume by about 30%.

The first stage is equipped with 13 engines and their individual thrust is also reduced compared to the NBP version. These benefits of densified propellants for RLV appear encouraging and within the continuation of this study densified propellants will continue to be investigated. Currently an expansion to densified LOx/LH2 and LOx/LC3H8 is planned. As mentioned in section 3.1, LC3H8 increases its density dramatically and thus launchers with this propellant could benefit even more from densification. Additional densification beyond the freezing point could lead to larger mass savings. These propellants are usually referred to as slush propellants and contain a certain mass fraction as solid particles. However, in order to estimate their effect on the launcher, detailed investigations of the propellant management subsystem have to be conducted and thus they were not included within these preliminary investigations.

*4.2.6 Preliminary results analysis for barge landing*

An overview of the preliminary sizing performed for barge landing and summarizing the results described in the previous subsections is presented in Fig. 9.

As expected the LOx/LH2 versions are much lighter than the hydrocarbon versions. For an upper stage ΔV of 6.6 km/s or 7.0 km/s, the LOx/LH2 launcher equipped with gas generator engines are about twice as light as their hydrocarbon counterparts, which are themselves very similar in term of mass. For an upper stage ΔV of 7.6 km/s, the hydrocarbon launchers are about three times as heavy as the LOx/LH2 launcher. Using a staged combustion engine allows to further decrease the GLOM of the LOx/LH2 by up to 25%. Densifying the propellant allows a reduction of the gross lift-off mass, due to better a structural index. It however stays about

60% over the GLOM of the LOx/LH2 counterparts, in the case of a LOx/LCH4 launcher.

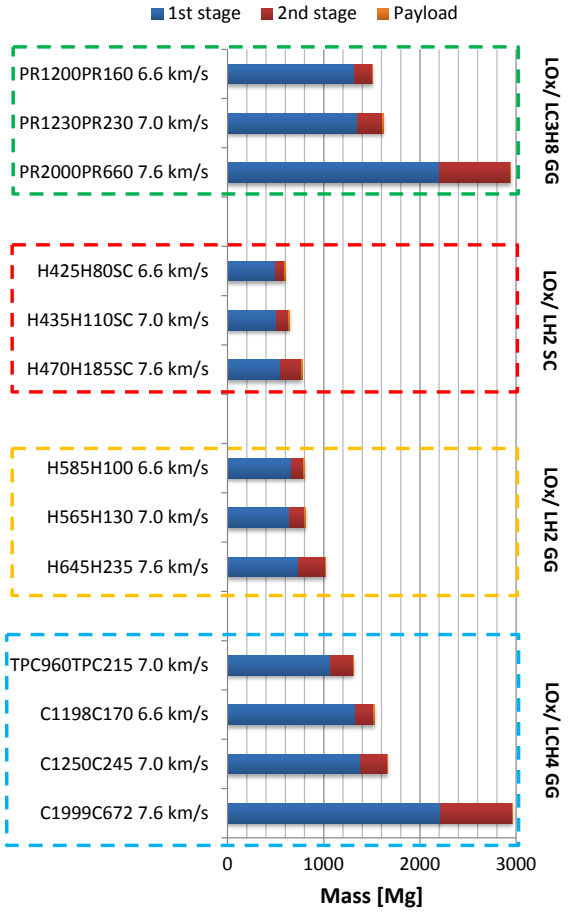


Fig. 9. Mass overview of the launchers performing DRL and sized based on structural indices derived from existing stages

As already observed previously, the GLOM of the launchers increases with increasing second stage ΔV. This is due to the fact that the second stage has to carry more propellant the more ΔV it has to deliver, thus making the stage heavier. This leads to a higher first stage mass and thus a higher launcher GLOM. To better understand the behaviour of launcher lift-off mass with increasing second stage ΔV, the second stage total masses for each propellant combination were used to interpolate second stage GLOMs as shown in Fig. 10. The curves shown were generated using the Tsiolkovsky rocket equation to estimate the initial to final mass ratio and then determine the stage dry mass by iteratively calculating the interpolated structural index (with the structural index formula from 3.3). The engine mass was estimated using a polynomial of second order fitted curve through the engine masses of the three different second stages (ΔV = 6.6, 7.0 and 7.6 km/s). The thus created curves fit well with the actual preliminary sized launchers for three different second stage ΔV values. As expected the second stage GLOM increases little for smaller ΔV, whereas it reaches prohibitive levels for a ΔV = 7.6 km/s. Note that the low mass increase domain corresponds to lower ΔV for the LOx/LCH4 and LOx/LC3H8 launch vehicles than for the LOx/LH2 launchers. This is explained by the fact that the structural index curve from Fig. 4 has a higher gradient for increasing propellant masses for LOx/LH2. As the mass of the second stage directly impacts the mass of the first stage; a high second stage ΔV is highly unfavourable due to high launch masses and thus high costs.

Independently of the propellant and the chosen engine type it appears that the launchers with an upper stage ΔV of 7.0 km/s are not much larger than those with a an upper stage ΔV of 6.6 km/s. The slope of the curves in Fig. 10 is indeed relatively small. As a consequence, due to the lower velocity at separation with a ΔV of 7.0 km/s for the upper stage, it is expected that the first stage is performing a descent under milder conditions, more favourable to reduce protection system and/or the refurbishment effort.

Fig. 10 also shows that LOx/LCH4 launchers seem to be generally heavier than the LOx/LC3H8 launchers although the specific impulse of LOx/LCH4 is slightly higher than that of the LOx/LC3H8 launchers.

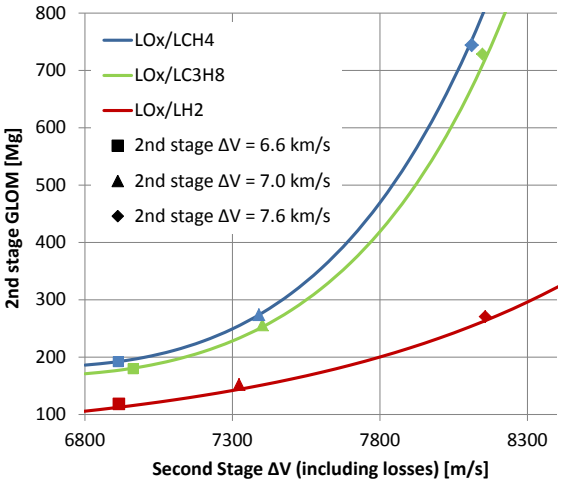


Fig. 10. 2nd stage GLOM (without payload) vs. 2nd stage ΔV for the LOx/LH2, LOx/LCH4 and LOx/LC3H8 launcher

*4.3 Safety aspects*

The choice between DRL and RTLS is also influenced by safety aspects. Compared with an expendable launcher, a partly reusable launch vehicle presents safety challenges. First of all, in the case of a RTLS mission, the return of the first stage towards the ground leads to additional risks, as failure could happen during this phase. An uncontrolled return or an explosion could endanger populations or facilities. Even

the ascent of a RTLS mission may present more risk than a classic ELV ascent trajectory. Indeed it is more efficient to have a more vertical ascent of the first stage, to reduce the propellant required for the RTLS return flight. This particularity can be observed in Fig. 11. The optimised ascent trajectory of H1000H250 in red can be compared with the flatter Ariane 5 ECA trajectory in blue. A more vertical trajectory increases the duration over the launch facilities and that combined with the increase of the debris footprint in case of failure increase the risks.

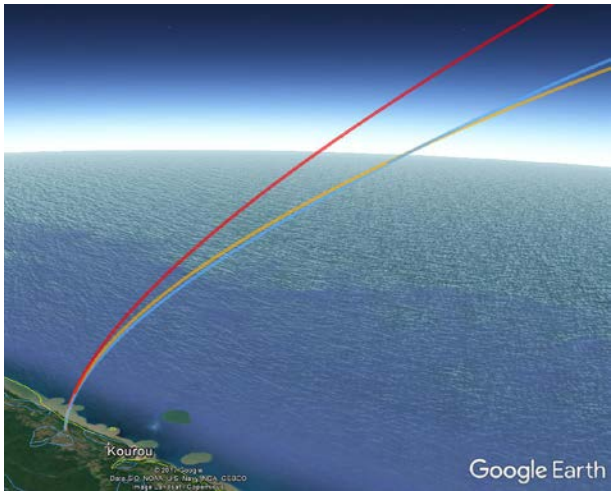

Fig. 11. Optimised ascent trajectories of H1000H250 (RTLS) in red, of H565H130 in yellow and Ariane 5 ECA in blue. (image generated with Google Earth, image data: Data SIO, NOAA, US Navy, NGA GEBCO, Landsat/Copernicus)

These aspects have been analysed by Martinez Torio et al. [20] for a smaller launch vehicle but can be extrapolated with a good confidence for the launcher presented in this paper. Note that to avoid these higher risks and guarantee the safety of the populations and facilities, the real trajectories will have to be modified. These modifications are however leading to a performance loss. As seen in Fig. 11, the H565H130 with a first stage performing a barge landing (DRL) has an ascent trajectory which is comparable with an Ariane 5 ECA launch. As a consequence, it can be expected that it is much easier to fulfil the safety requirement with such a concept. The landing operation in the middle of the ocean is also not expected to present major challenges from a purely safety point of view.

These findings together with the high GLOM found in the preliminary sizing for the RTLS concepts led to focus first on barge landing configurations for more detailed preliminary design of selected concepts during the second iteration.

## 5. Selected configurations for the second iteration

The study of the preliminary sized launchers using an interpolated structural index as described in section 4.2 lead to the conclusion that launchers with a second stage ΔV of 7.0 km/s seem to be the most favourable configuration for the VTOL concept with DRL. Lower upper stage ΔV are leading to slightly lower GLOM, but the first stage descent is expected to be harsher, due to the higher separation velocity. The respective LOx/LH2 and the LOx/LCH4 launcher (both with gas generator engines) were subjected to a more detailed analysis of the stage masses and the launcher's performance. Indeed the method of estimating the stage masses via pre-assumed structural index is not taking into account the specificity of the vehicle and the particular chosen architecture.

### *5.1 Launch vehicle model*

A more detailed preliminary mass model was set up to calculate the launcher masses. The mass model takes the structure, the propellant system, the engines and several other subsystems into account. The structural masses of the tanks, the interstage, the second stage front skirt and the first stage rear skirt were calculated using the tool *lsap*. Load cases taken from the flown trajectory are used for the structural sizing and consequently to determine the masses of the respective components. For both stages and each propellant combination common bulkhead tanks have been selected to keep the structural mass and consequently the vehicle mass as low as possible. The tanks and skirts were simulated as stiffened cylinders made of an aluminium alloy (AA2219) where the number of stringers and frames ("Z" shaped) is subject to an optimization to determine the lightest final configuration possible. The tanks are pressurized at 3 bar. It is important to note that this value was chosen based on experience and is subject to optimization in future work. The interstage was modelled as fully aluminium honeycomb structure. The safety factor was chosen to be 1.25, a standard value for unmanned launchers. The propellant system was modelled using the tool *pmp*. This tool was used to determine the tank sizes and the masses of the propellant supply and pressurization system. For the LOx/LH2 launcher, a cryogenic insulation is considered for both tanks. It is mounted on the inside of the tank and then covered with a thin aluminium foil as liner [21]. Internal insulation avoids damage to the insulation during re-entry by hot combustion gases. Note however that the TRL of such insulation is still low.

The subsystems were calculated using partly formulas included in the mass estimation tool *stsm* and partly by scaling systems of the Ariane launchers to the respective launcher size. The landing legs and grid fins were linearly scaled using the empty mass of the

Falcon 9. This method is a conservative approach and probably leads to overestimated masses. This was confirmed by preliminary calculations with a simplified structural model. For future studies a more detailed estimation of the landing leg and grid fin mass shall be implemented in the rocket model. The engines were modelled as described in section 3.2. The structure, subsystems and cryogenic insulation of the reusable first stage are subjected to an additional margin of 14%, whereas the margin for the engines is 12%. The second stage margin is 10% for all systems. The margin for the second stage is lower since it is not a reusable stage and therefore has a higher TRL.

*5.2 Results*

The results of the analysis of the LOx/LH2 and the LOx/LCH4 launcher with more detailed mass model are presented in Table 5. Both launchers show a great decrease in GLOM of about 45% compared to the results of the first iteration modelled with pre-assumed structural index. This decrease can mainly be explained by the overestimation of the second stage dry mass by using the structural index method. The problem with the extrapolation method of the structural index is the fact that the second stages are relatively large and in a tankage domain corresponding to existing first stages. However, the structural indices of first stages tend to be higher than the respective indices of upper stages as they have to carry an upper stage on top and withstand higher bending loads. This leads to an overestimation of the second stage dry mass which in the further course leads to a higher first stage mass and thus a heavier launcher.

Table 5. LOx/LH2 and LOx/LCH4 launchers with detailed preliminary mass model for a second stage ΔV = 7.0 km/s

| **Component** | | **H298H77** | **C648C142** |
|---|---|---|---|
| **1st stage** | | | |
| Dry mass | [Mg] | 43.6 | 60.1 |
| Ascent propellant | [Mg] | 280.0 | 620.8 |
| Descent propellant | [Mg] | 18.0 | 27.2 |
| Engine number | [-] | 9 | 11 |
| M sep | [-] | 9.92 | 9.77 |
| F_vac | [kN] | 7000 | 13900 |
| GLOM 1st stage | [Mg] | 348.0 | 721.0 |
| **2nd stage** | | | |
| Dry mass | [Mg] | 8.5 | 10.8 |
| Ascent propellant | [Mg] | 77.0 | 157.0 |
| F_vac | [kN] | 850 | 1390 |
| GLOM 2nd stage (w/o P/L) | [Mg] | 88.2 | 157.1 |
| **GLOM Launcher** | **[Mg]** | **443.7** | **885.6** |
| **P/L** | **[kg]** | **7454** | **7490** |
| **Diameter** | **[m]** | **5.2** | **5.5** |
| **Length** | **[m]** | **82** | **75.3** |

The LOx/LH2 launcher is about half the mass of the LOx/LCH4 launcher. This relation could also be observed in the first iteration, which is an indication that the relative results of the first iteration are up to a certain extent still valid even if the pre-assumed structural index were too pessimistic. The LOx/LH2 launcher has a GLOM that is less than that of the Falcon 9 (550 tons), while delivering about two tons additional payload into GTO (7500 kg vs 5500 kg of Falcon 9). However, due to the fact that hydrogen has a much lower density than RP-1 the LOx/LH2 launcher is larger, see Fig. 12. The LOx/LH2 launcher and Falcon 9 both have 9 engines.

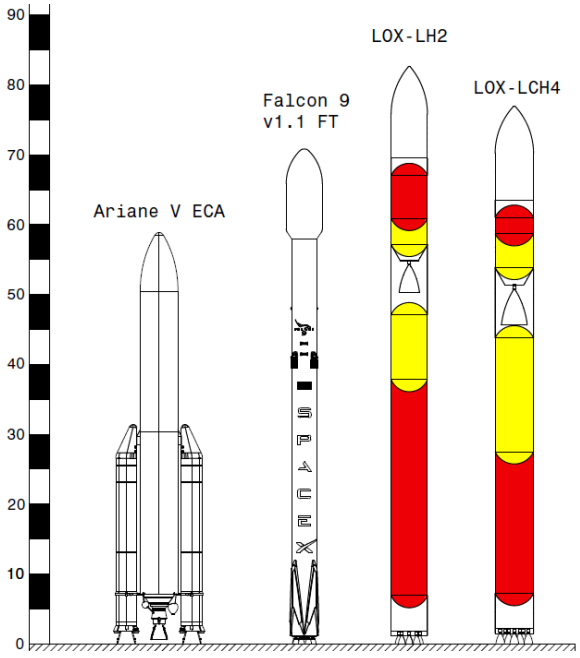


Fig. 12. Ariane 5, Falcon 9, H297H77 and C648C142 (from left to right) launchers inner & outer geometry

The LOx/LCH4 launcher has a mass at lift-off of 884 tons and has 11 engines. Due to the difficult accommodation of the engines, the diameter of the launcher had to be set to 5.5 m, the minimum possible to fit all 11 engines within the rear skirt. Furthermore, the second stage engine barely fits in the interstage, so in future studies the interstage length should be increased. Due to the higher density of methane, the C648C142 launcher is almost of the same volume as the LOx/LH2 launcher. The payload capability is about 7500 kg which is less than the announced 13 tons to GTO of the LOx/LCH4 launcher "New Glenn" that is currently under development at Blue Origin [22]. However, the New Glenn is about 76% bigger (regarding total volume) than the VTOL methane launcher, presented here. No official masses have been published by Blue Origin so far, but considering the thrust at lift-off (7 BE-4 engines with a total thrust of

17.1 MN) and a minimum T/W ratio of 1.2, the lift-off mass should be in the range of 1250 to 1450 tons. Comparing this lift-off mass with those of the first and second iterations of 1667 tons and 884 tons, respectively, confirms that the second iteration results are realistic. The second iteration LOx/LH2 and LOx/LCH4 launchers are plotted alongside the Ariane 5 and the Falcon 9 in Fig. 12 in order to get a feeling for the size of the proposed systems.

## 6. Aero-thermal analyses of the descent

In order to assess the aero-thermal conditions during the descent, the descent trajectory of the H565H130 defined in 4.2.1 has been considered. The re-entry boost is studied for several freestream conditions using computational fluid dynamics (CFD). The aerothermal analysis follows the concepts detailed in a previous study [9] on the thermal loads of the Falcon 9 side wall.

### *6.1 TAU CFD solver*

All numerical investigations for the aero-thermal analysis of the descent were performed using the hybrid structured/unstructured DLR Navier-Stokes solver TAU. This DLR developed solver is validated for a wide range of steady and unsteady sub-, trans- and hypersonic flow cases. The TAU code is a second order finite-volume solver for the Euler and Navier-Stokes equations in the integral form using eddy-viscosity, Reynolds-stress or detached and large eddy simulation for turbulence modelling. For the presented investigations, the Spalart-Allmaras one-equation eddy viscosity model [23] was used. The AUSMDV flux vector splitting scheme was applied together with MUSCL gradient reconstruction to achieve second order spatial accuracy. The applied model for thermodynamic and transport properties are based on a non-reacting mixture of thermally perfect gases (air and engine exhaust) and are derived from the CEA thermodynamic and transport databases.

### *6.2 Engine model and fluid composition*

In order to model the engine exhaust gas composition, equilibrium conditions for H2/O2 at engine combustion chamber pressure conditions were determined and isentropically expanded to throat conditions using Cantera [24]. This gas composition is then used to create a thermally perfect pseudo gas for 2D axisymmetric nozzle and exterior vehicle exhaust calculations. The chamber total gas density after tweaking match the Isp of the nozzle with the engine parameters within 1.5 %.

### *6.3 Retro-propulsion trajectory*

The retro-propulsion phase starts at approximately 68 km and exposes the vehicle to Mach numbers between 9.45 and 4.5. For the purpose of this study several trajectory points were investigated using CFD, assuming steady state flow conditions. The retro-boost trajectory and the trajectory points studied in detail are shown in Fig. 13 (solid line) and Table 6.

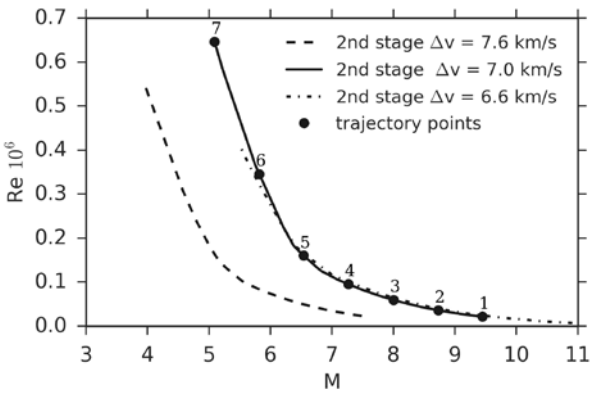


Fig. 13. Retro-propulsion trajectories within M-Re number space

Table 6. Main retro-propulsion trajectory points of configuration H565H130 (upper stage ΔV = 7.0 km/s)

| Traj. Point | t [s] | h [km] | M | Re x10$^6$ |
|---|---|---|---|---|
| 1 | 243.0 | 68.0 | 9.45 | 0.0212 |
| 2 | 247.0 | 63.3 | 8.73 | 0.0361 |
| 3 | 252.0 | 58.5 | 8.00 | 0.0595 |
| 4 | 257.0 | 53.6 | 7.27 | 0.0952 |
| 5 | 263.0 | 48.3 | 6.54 | 0.1604 |
| 6 | 271.0 | 42.1 | 5.82 | 0.3456 |
| 7 | 278.0 | 36.9 | 5.09 | 0.6461 |

### *6.4 Plume-body interaction*

A number of RANS computations covering the entire trajectory of the retro propulsion manoeuvre at an angle of attack = 0° were carried out. The computational domain is based on a quarter slice geometry and does not contain combustion chamber or nozzle geometry. The exhaust gas is modelled as described in the previous section (6.2) and is imposed onto the three active engines as a Direchlet boundary condition. The freestream gas is modelled as thermally perfect air. The side wall heat flux, plume structure and aerodynamic drag are investigated for the exemplary trajectory points. A detail view of the computational domain and the active engine configuration for the quarter slice are shown in Fig. 16.

The total drag coefficients and the viscous drag contribution are shown in Fig. 14. At high altitudes the plume is heavily over-expanded, leading to flow reversal and negative skin friction drag on the launcher side walls, reducing overall drag. Schematics of the flow field structure and plume extension at three different trajectory points are shown in Fig. 15. The spreading of the plume is considerably reduced as the atmospheric density increases. The heat flux distribution is widely uniform at high altitudes when the vehicle is

completely submerged in its exhaust plume. With decreasing altitude the plume extent is reduced, leading to higher heat flux magnitudes near the engine side of the launcher stage. The flow structure of the plume is highly three dimensional due to the asymmetric active engine configuration and results in an asymmetric heat flux distribution especially at lower altitudes.

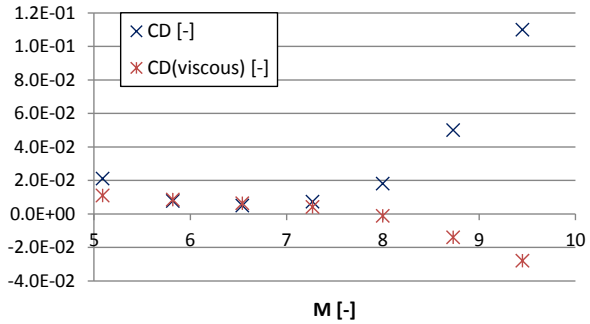


Fig. 14. Drag coefficient (excluding thrust) for launcher stage during retro-propulsion for $T_{wall}$ = 300 K

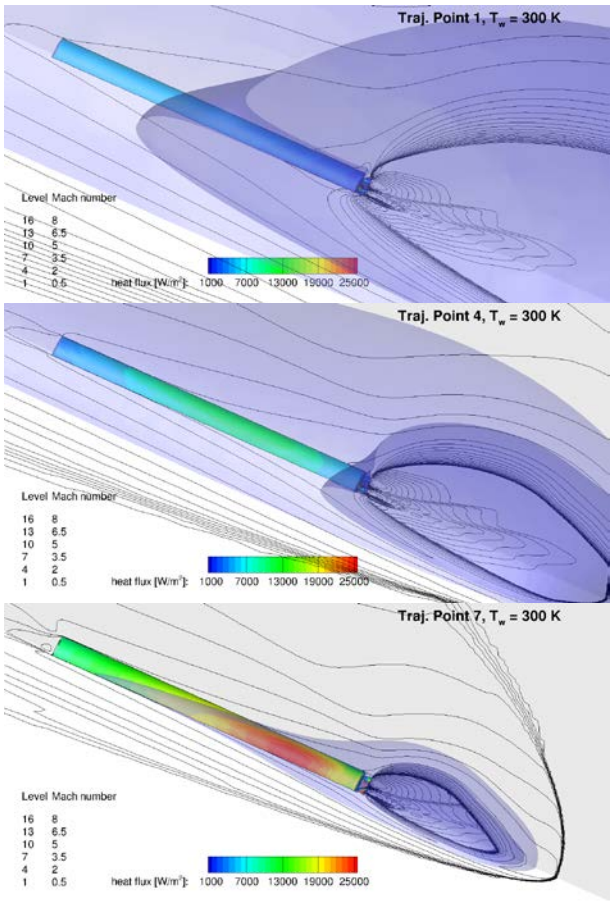


Fig. 15: Plume-body interaction on several trajectory points. Contour shows wall heat flux (for $T_{wall}$ = 300 K), line contour shows Mach number on X-Y and X-Z plane. Engines are operating on X-Z plane (angle = 90 deg). Plume iso-surface (blue) shows engine exhaust mass fraction of 0.3, (dark-blue) exhaust mass fraction of 0.7.

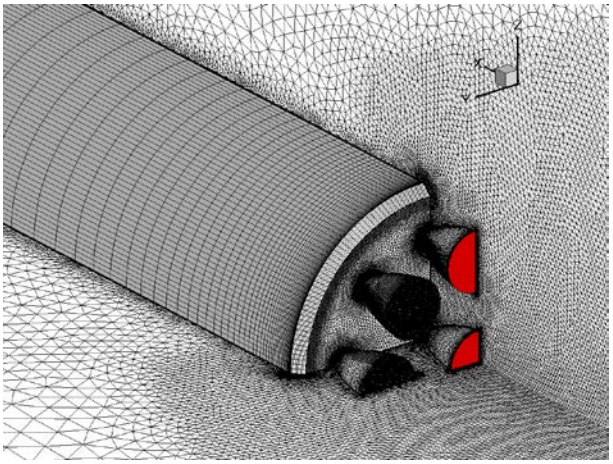

Fig. 16: Detail of computational domain and coordinate system. Red planes indicate active engines

*6.5 Aerothermal analysis*

The heat flux distribution is strongly dependent on the extension of the plume and therefore on the trajectory position. Hence a number of computations are needed to create an aerothermal database. The database is built on the previously described trajectory points as well as supporting points close to nonlinear trends within the Mach and Reynolds number conditions studied. The Mach and Reynolds number are used to describe the physical parameter space enabling interpolation using physical parameters instead of the time domain. For each database point CFD calculations at constant wall temperature of 300 and 400 K were performed. The final aerothermal database consists of the linearly interpolated heat flux as a function of trajectory time and sidewall coordinate. A previous study by Ecker et al. [9] estimated the error of the interpolated data to be within 3.2 % and 10 % for a worst case scenario.

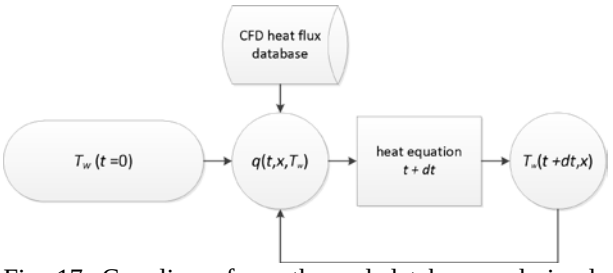


Fig. 17: Coupling of aerothermal database and simple lumped mass model

A simple lumped mass model without heat conduction between elements is used to estimate the wall temperature during the retro-propulsion manoeuvre. For this purpose the casing is modelled as a

number of thin aluminium segments of variable thickness, for each of which a 0 D heat equation is solved using an Euler scheme. The coupling between the aerothermal database and the integration algorithm is shown in Fig. 17 The skin thickness distribution, resulting from the preliminary structural design, is shown in Table 7 and used to determine element mass along the side wall for the lumped mass model calculations. Note that the stiffening elements have been neglected in the lumped mass model. The initial condition and material parameters are summarized in Table 8.

Table 7: Skin surface thickness of launcher stage sections

| Section | Length | Skin thickness |
|---|---|---|
| Rear skirt | 5.750 m | 3.0 mm |
| Lower stage LH2 tank | 38.485 m | 1.8 mm |
| Lower stage LOx tank + interstage | 12.765 m | 3.4 mm |

Table 8: Material parameters for Aluminium alloy AA2219T87 and starting conditions for lumped mass model

| Parameter | Value |
|---|---|
| $C_p$ | 0.858E+3 J/kgK |
| density | 2840 kg/m$^3$ |
| T(t = 0s) | 300 K |

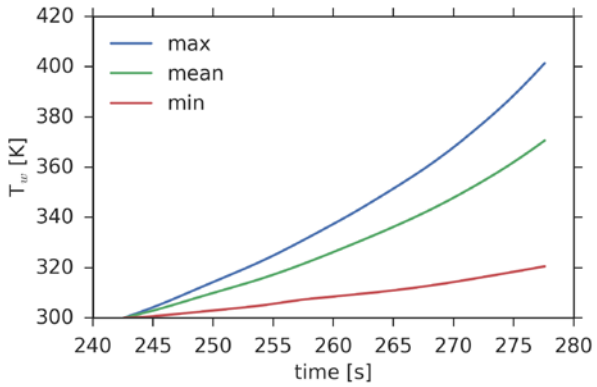


Fig. 18: Time dependent surface mean, minimum and maximum temperature on the launcher sidewall during the retro-propulsion boost

The time dependent surface temperature distribution is shown in Fig. 19. As expected the critical section with high surface temperatures is the LH2 tank with its low skin thickness. With the plume retracting towards the rear during the later stages of the retro-boost phase, the maximum temperatures are found in the central section of the LH2 tank side wall. The maximum, mean and minimum surface temperatures during retro-propulsion are shown in Fig. 18. The maximum temperature reaches slightly above 400 K and should be considered a worst case scenario as no heat transfer to and from the tank contents, as well as to and from the stiffening elements is considered. In average the stage wall temperature is increasing to 360 K with some areas as cold as 320 K.

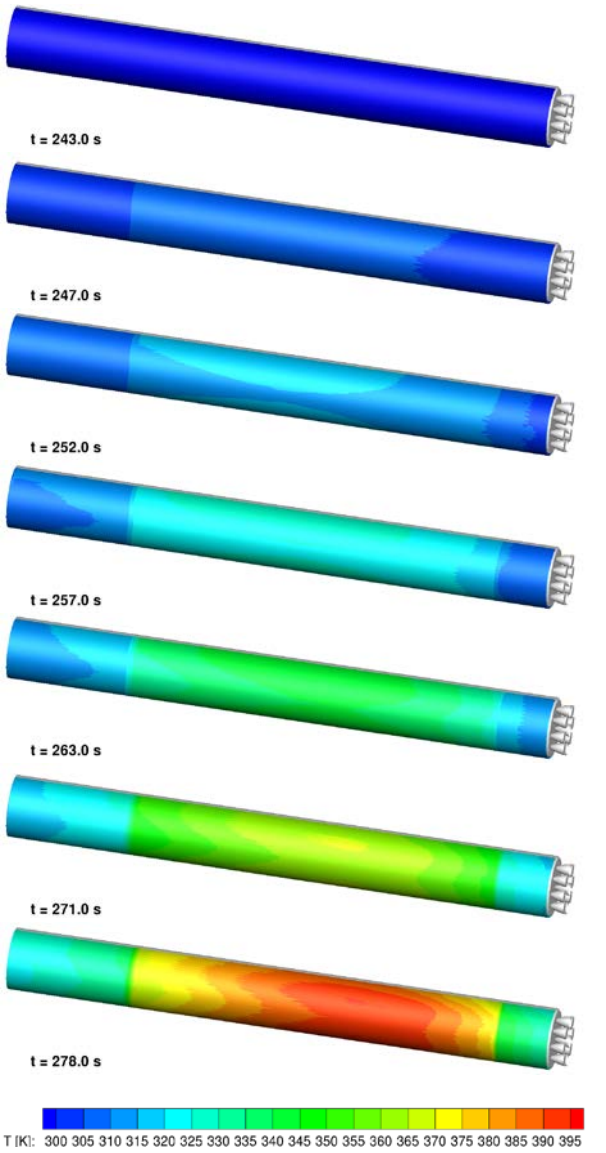


Fig. 19: Time dependent surface temperature distribution on the launcher sidewall shown at seven different trajectory points

The heat flux on the sidewall changes significantly after the retro-propulsion manoeuvre is carried out. Computation results are shown in Fig. 20. The heat flux on the side wall of the LH2 and LOx tanks decreases strongly, while the maximum heat flux on the lower skirt, baseplate and nozzles increases. The secondary flow around the nozzle geometry after the detached

shock in front of the vehicle leads to a pattern of heat flux peaks on the lower skirt geometry.
Note that in reality, the landing legs would cover at least part of the lower skirt. Thermal protection would be probably required in this region.

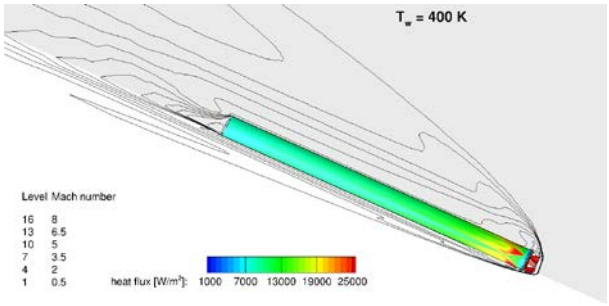


Fig. 20: Flow field around the launcher stage about 5.5 s after the retro-propulsion manoeuvre ended (altitude 32.51 km, Mach number 5.24, time 283.4 s)

When considering the first stage return trajectories for the staging corresponding to an upper stage ΔV of 6.6 km/s and 7.6 km/s for the LOx/LH2 GG versions (see Fig. 13) some preliminary conclusions may be drawn. Both the trajectory with upper stage ΔV of 7.0 and 6.6 km/s have similar retro-propulsion flow regimes. As the 6.6 km/s variant enters the manoeuvre at higher Mach numbers and lower Re numbers and also exits at higher Mach numbers and lower Re numbers, the thermal loads on the tanks are likely to be lower and the thermal loads on the lower skirt, baseplate and leg structures are likely to be higher when compared to the 7.0 km/s variant. The 7.6 km/s configuration has a very different retro-propulsion trajectory with generally lower Mach numbers, leading to generally lower stagnation temperatures and lower thermal loads during the non-propulsive phase. However, it should be noted that the integrated thermal loads depend on the trajectory as a whole and may not be entirely deduced from this analysis. This first comparison also shows that some freedom exist in the choice of the return trajectory. This has a strong influence on the heat loads and therefore on the optimal stage design and thermal protection concept, if needed. Refurbishment effort and consequently costs are also related to these aspects.

## 7. Conclusions

Within this paper two different methods were deployed in order to parametrically investigate different VTOL concepts. First a large number of generic launchers were pre-designed using structure indices derived from existing stages. The following trends and results were identified:

- RTLS does not seem adapted to GTO missions in the case of a TSTO launch vehicle achieving 7.5 tons payload performance. The ΔV required to perform the RTLS is really high. The propellant for the related manoeuvres has to be carried during ascent leading to huge launcher with limited economic relevance. Performing a more detailed preliminary analysis based on loads for the structural sizing would allow for a significant reduction of the launch vehicle gross lift-off mass. It is however still expected to be very high.
- Performing down-range landings leads to much more acceptable designs, with interesting results for upper stage ΔV in the range of 6.6 to 7.0 km/s.
- Although LOx/LC3H8 is characterised by a lower specific impulse than LOx/LCH4, the higher density of LC3H8 lead to slightly lighter and consequently compacter launchers.
- Without propellant densification LOx/LCH4 launcher are slightly bulkier than LOx/LH2 launch vehicles.
- Independently of the propellant, the number of engines in the first stage has a strong influence on the launcher performance, even for constant lift-off thrust to weight ratio. Indeed, a small number of engines implies that they are large. Depending on the size of the upper stage this could be penalizing due to the high mass of the engine or beneficial since it limits the gravitational losses. Similarly for the descent, large engines usually help to reduce losses while they may have difficulties landing with a thrust to weight ratio near 1. Minimum throttling level and risk of flow separation in the nozzle can be limiting factors.

In a second iteration, more detailed preliminary analyses were performed for selected designs and resulted in the following findings:

- The launchers calculated with a more detailed structural and mass preliminary model during the second iteration are about half as heavy as the preliminary launchers calculated via pre-assumed structural index, during the first iteration. This is due to the fact that structural index curves for propellant loading in the range of the large second stages studied here are mainly influenced by existing first stages. The load that first stages and second stages have to withstand are however of different nature.
- The respective LOx/LH2 launcher with an upper stage ΔV of 7.0 km/s is lighter than a Falcon 9 and delivers 2 tons more payload to GTO (7500 kg vs 5500 kg) in DRL mode.
- The loads encountered by the first stage during the descent to the barge do not influence the structural design significantly as the tanks are almost empty and bending moments are reduced without upper stage and fairing. Analyses showed that the first stage can withstand much higher

axial and lateral loads and dynamic pressure during the descent than during ascent, without influence on the structure mass, see [26].
- The LOx/LH2 launcher has a smaller volume than the LOx/LCH4 launcher.

When the aerothermal loads are considered the following conclusions can be drawn:

- The engine exhaust during the retro-propulsion phase strongly influences the flow around the stage leading to a significant modification of the drag.
- Depending on the chosen descent trajectory the aerothermal loads could be critical for the structure without thermal protection. Results of a simplified skin thickness based mass model to estimate wall temperatures on the launcher sidewall during the retro-propulsion manoeuvre show that the low wall thickness of the LH2 tank combined with localized high heat flux at the end of the re-entry manoeuvre leads to increased wall temperatures (up to about 400 K in the worst case). Such analyses of the retro-propulsion phase help to tweak the descent trajectory to guarantee that thermal protections on the tank walls are not needed.
- A first numerical study of the heat flux on the trajectory after the retro-propulsion phase shows regions with high heat flux to occur at the lower skirt, baseplate and nozzle section. As this section is also an attachment point for the landing leg structure, additional studies considering the landing legs geometry should be performed. This flight phase is most relevant for the thermal protection dimensioning on those structures.
- The thermal loads during both the retro-propulsion and the subsequent ballistic phases are strongly dependant on the chosen trajectory. The aerothermal analysis provided may be used to select or optimize the descent trajectory. Depending on the performance requested, a less performance optimized trajectory could reduce the loads on the vehicle and consequently increase its life time or reduce the refurbishment efforts.

Within the continuation of this study it is planned to continue refining the preliminary sizing for the different propellant combinations. Critical sub-systems will be the object of more detailed analysis. The final goal is to compare expected launch service costs for the different concepts. For this purpose a better knowledge of aspects related to the operational concept or refurbishment efforts between two flights is needed. It can only be validated with the help of demonstration flights. With this in mind, the two largest contributors to the European launcher program, CNES and DLR have initiated a common project called CALLISTO (Cooperative Action Leading to Launcher Innovation in Stage Toss back Operations) aiming at flying a reusable reduced scale first stage rocket demonstrator performing vertical take-off and landing [25].

At the level of the systematic first stage reusability comparison, work will be continued for winged concept, as well. A first overview comparing the results for a retro-propulsion methods and winged methods has been prepared by Sippel et al. [26].

**Acknowledgements**

This work has been performed within the X-TRAS project funded by DLR.

The authors would also like to acknowledge the contribution of Mr. Matthieu Delbourg for the CAD model and of Mr. Alexander Kopp for the structural analysis.

**References**

[1] M. Sippel, C. Manfletti, H. Burkhardt, Long-term/strategic scenario for reusable booster stages, Acta Astronautica, Volume 58, Issue 4, February 2006, pp 209-221, DOI: 10.1016/j.actaastro. 2005.09.012

[2] Patentschrift (patent specification) DE 101 47 144 C1, Verfahren zum Bergen einer Stufe eines mehrstufigen Raumtransportsystems, released 2003.

[3] M. Sippel, J. Klevanski, Progresses in Simulating the Advanced In-Air-Capturing Method, 5th International Conference on Launcher Technology, S15.2, Madrid, November 2003.

[4] D. C. Freeman, T. A. Talay, R. Eugene Austin, Single-stage-to-orbit — Meeting the challenge, Acta Astronautica, Volume 38, Issue 4, 1996, pp. 323-331, ISSN 0094-5765, http://dx.doi.org/ 10.1016/0094-5765(96)00051-3.

[5] A. Koch, M. Sippel, A. Kopp, A. van Foreest, C. Ludwig and T. Schwanekamp, Critical analysis of Falcon 1, 1e, Falcon 9 and Dragon capsule, SART TN-018/2010, 2010.

[6] M. R. Bhagat, SpaceX Falcon 9 v1.1, Falcon Heavy remodelling; Falcon 9 v1.1 descent trajectory and performance optimization, SART TN-020/2014, 2014.

[7] J. Pouplin and E. Dumont, Falcon 9 v1.1 and v1.2 performances and first stage descent/return trajectories analyses, DLR-IB-RY-HB-2016-51, SART TN-009/2015, 2015.

[8] S. Stappert and E. Dumont, Reusability of launcher vehicles by the method of SpaceX, SART TN-007/2016, 2016

[9] T. Ecker, S. Karl, E. Dumont, S. Stappert, D. Krause, A Numerical Study on the Thermal Loads During a Supersonic Rocket Retro-Propulsion Maneuver, AIAA 2017-4878, 53rd AIAA/ SAE/ASEE Joint Propulsion Conference, 2017 AIAA Propulsion and Energy Forum and Exposition, Georgia, USA, 10-12 July 2017, DOI: 10.2514/6.2017-4878.

[10] L. Bussler, M. Sippel, Comparison of Return Options for Reusable First Stages, AIAA 2017-2137, 21st AIAA International Space Planes and Hypersonics Technologies Conference, Xiamen, China, 6-9 March 2017, DOI: 10.2514/6.2017-2137.

[11] J. Wilken, E. Dumont, S. Stappert, New features of tosca and rts in version 1.33, SART-TN003/2017.

[12] H. Burkhardt, M. Sippel, A. Herbertz, J. Klevanski, Comparative Study of Kerosene and Methane Propellant Engines for Reusable Liquid Booster Stages, 4th International Conference on Launcher Technology "Space Launcher Liquid Propulsion", Liège, Belgium, 3-6 December 2002.

[13] D. Haeseler, V. Bombelli, P. Vuillermoz, R. Lo, T. Marée, F. Caramelli, Green Propellant Propulsion Concepts for Space Transportation and Technology Development Needs, 2nd International Conference on Green Propellants for Space Propulsion (ESA SP-557), Chia Laguna, Italy, 7-8 June 2004.

[14] R. F. Barron, G. F. Nellis, Cryogenic Heat Transfer, Second Edition, CRC Press, 2016, ISBN 9781482227444.

[15] Air Liquide, Gas Encyclopedia Air Liquide, https://encyclopedia.airliquide.com/, as accessed on June 19, 2017.

[16] P. Caisso, P. Brossel, T. Excoffon, M. Illig, T. Margat, Development Status of the Vulcain 2 Engine, AIAA 2001-3550, 37th AIAA/ ASME/ SAE/ ASEE Joint Propulsion Conference & Exhibit, Salt Lake City, USA, 8-11 July 2001, DOI: 10.2514/6.2001-3550.

[17] R. Yamashiro, M. Sippel, Preliminary Design Study of Staged Combustion Cycle Rocket Engine for SpaceLiner High-Speed Passenger Transportation Concept, IAC-12-C4.1.11, 62nd International Astronautical Congress 2011, Cape Town, South Africa, 3-7 October, 2011.

[18] G. Waxenegger, J. Riccius, E. Zametaev, J. Deeken, J. Sand, Implications of Cycle Variants, Propellant Combinations and Operating Regimes on Fatigue Life Expectancies of Liquid Rocket Engines, 7th European Conference for Aeronautics and Space Sciences, Milan, Italy, 3-6 July, 2017.

[19] J. Deeken, D. Suslov, N. Rackemann, A. Preuss, Combustion Performance and Stability of a Porous Injector Compared with a State of the Art Coaxial Injector, SP2014-2969154, Space Propulsion 2014, Cologne, Germany, 19-22 May, 2014.

[20] A. Martinez Torio, J.M. Bahu, D. Delorme, V. Guenard, H. Poussin, Near range safety analysis for a reusable launcher concept based on toss-back, The Journal of Space Safety Engineering, Volume 4, Issue 1, March 2017, pp. 29-35, DOI: 10.1016/ j.jsse.2017.02.006.

[21] W. Fischer, Development of Cryogenic Insulations for Launcher Upper Stages, ICES-2014-142, 44th International Conference on Environmental Systems, Tucson, USA, 2014, 13-17 July.

[22] Blue Origin, https://www.blueorigin.com/new-glenn, as accessed on September 15, 2017.

[23] P. R. Spalart, S. R. Allmaras, A One-Equation Turbulence Model for Aerodynamic Flows, AIAA-92-0439, 30th Aerospace Sciences Meeting and Exhibit, Reno, USA, 1992, 6-9 January. DOI: 10.2514/6.1992-439.

[24] D. G. Goodwin, H. K. Moffat, R. L. Speth, Cantera: An Object-oriented Software Toolkit for Chemical Kinetics, Thermodynamics, and Transport Processes," 2017, Version 2.3.0.

[25] P. Tatiossian, J. Desmariaux, M. Garcia, Callsito Project – Reusable first stage Rocket Demonstrator, 7th European Conference for Aeronautics and Space Sciences, Milan, Italy, 3-6 July, 2017.

[26] M. Sippel, S. Stappert, L. Bussler, E. Dumont, Systematic Assessment of a Reusable First-stage Return Options, IAC-17-D2.4.4, 68th International Astronautical Congress, Adelaide, Australia, 25-29 September 2017.